

# A unified formula for calculating bending capacity of solid and hollow concrete-filled steel tubes under normal and elevated temperature

Min Yu<sup>a,c</sup>, Xiaoyan Pei<sup>a</sup>, Lihua Xu<sup>a</sup>, Jianqiao Ye<sup>a,b,\*</sup>

a. School of Civil Engineering, Wuhan University, Wuhan 430072, China;

b. Department of Engineering, Lancaster University, Lancaster, LA1 4YR. UK;

c. Engineering Research Center of Urban Disasters Prevention and Fire Rescue Technology of Hubei Province, Wuhan 430072, China;

**Abstract:** Bending is one of the most common forms of deformation that may cause failure of a structural member, such as a column, especially when the member is exposed to fire. Fire resistance design is therefore an important factor that must be considered in the design process of modern building structures. Based on the authors' previous work on the unified formulation of axially loaded CFST hollow and solid columns with circular and polygonal sections, a unified formula for calculating the ultimate bending moment of solid and hollow CFST columns at room temperature is proposed first in this paper. The formula is then extended to include elevated temperature using the average temperature method. Finally, a unified formula for both room and elevated temperature are presented. Validations are carried out through comparisons with the results from experimental tests and finite element simulations.

**Keywords:** Concrete-filled steel tube (CFST); Ultimate Bending Moment; Average temperature; Unified method;

## Notations

$M_u, M_{u,T}$	ultimate bending moment of CFST section at room and elevated temperature, respectively
$A_s, A_c, A_k$	area of steel, concrete and hollow, respectively
$\psi$	hollow ratio, $\psi = A_k / (A_c + A_k)$
$n$	number of edges, (infinite for circular cross section)
$f_{ck}, f_{ck,T}$	Prism compressive strength of concrete at room and elevated temperature, respectively
$f_y, f_{y,T}$	characteristic strength of steel at room and elevated temperature, respectively
$\xi$	confining coefficient at normal temperature, $\xi = A_s f_y / A_c f_{ck}$
$\xi_{sc}$	solid confining coefficient at normal temperature, $\xi_{sc} = A_s f_y / (A_c + A_k) f_{ck} = \xi(1 - \psi)$
$\xi_T$	confining coefficient at elevated temperature, $\xi_T = A_s f_{y,T_s} / A_c \bar{f}_{ck,T_c}$
$\bar{T}_s, \bar{T}_c$	average temperature of steel tube and concrete core, respectively
$k_{s,T}, k_{c,T}$	reduction factor of strength of steel and concrete, respectively
$\bar{k}_{c,T}$	equivalent reduction factor of strength of concrete
$f_{y,T_s}$	equivalent strength of steel tube at $\bar{T}_s$
$\bar{f}_{ck,T_c}$	equivalent strength of concrete core at $\bar{T}_c$

$R, D$	Radius and dimension of circular steel tube, $D = 2R$
$\bar{R}, \bar{D}$	Equivalent radius and dimension of square steel tube, $\bar{D} = 2\bar{R}$
$B$	Side length of square steel tube
$t$	Thickness of steel tube
$F_{st}, M_{st}$	Composite force of steel part on tensile side and the corresponding bending moment
$F_{st}, M_{sc}$	Composite force of steel part on compression side and the corresponding bending moment
$F_{cc}, M_{cc}$	Composite force of concrete part on compression side and the corresponding bending moment

## 1 Introduction

Concrete-filled steel tubes (CFST) columns have been used widely in modern construction industry as they offer several distinct advantages in terms of both structural performance and construction sequence. Fire design of a CFST column is one of the most important factors that must be considered in its design process<sup>[1]</sup>. Current research on static performance of CFST columns includes testing, modelling and calculation of the columns subjected to axial compression<sup>[2-9]</sup>, pure bending<sup>[10-14]</sup> and combined load<sup>[15-17]</sup>. Some calculation methods have also been proposed to estimate fire resistance of CFST columns under compression. Kodur<sup>[18]</sup> conducted parametric analysis through experiments and numerical calculations, and proposed formulas for calculating fire resistance time of solid circular and square CFST columns using a regression analysis; Li et al.<sup>[19]</sup> proposed a formula for evaluating load bearing capacity of solid circular CFST columns under fire on the basis of also a parametric and regression analysis; Tan and Tang<sup>[20]</sup> applied the Rankine method to the analysis of reinforced and plain solid CFST columns at elevated temperature; Espinos et al.<sup>[21,22]</sup> presented a simple calculation method for evaluating fire resistance of circular and elliptical solid CFST columns based on Eurocode 4<sup>[23]</sup>, where the concept of equivalent temperature was adopted. A unified method for calculating fire resistance of solid and hollow CFST columns under axial load was reported by Yu, et al<sup>[24]</sup>. Instead of carrying out a coupled heat transfer and mechanical analysis, the method requires calculation of average temperature only, which significantly simplifies the solution process. Comparisons with experimental results have shown that the method is sufficiently accurate and reliable.

When a column is subjected to loading, bending may occur. It can be seen from the above literature review that there is already extensive research on static performance of CFST columns under pure bending. However, the research on fire resistance of CFST columns under pure bending is relatively rare. There are certainly requests from the construction community for further research and better understanding of this important structural behavior.

Built on the success in utilizing average temperature in the fire resistance analysis of CFST columns subjected to axial loads<sup>[24]</sup>, this paper attempts to develop a design equation for the fire resistance of CFST columns under pure bending by incorporating the average temperature approach developed previously by the authors. The design equation will be presented in a unified form that can be used to calculate bending capacity of CFST columns at both room and elevated temperature.

## 2 Bending capacity of concrete-filled steel tube at room temperature

### 2.1 Limit analysis of CFST cross-sections under pure bending

In the following sections, limit analysis approach is followed to calculate the ultimate bending capacities of solid and hollow CFST sections on the basis of the following assumptions: 1) The tension resistance of the

concrete is negligible, and the maximum stress the concrete in compression can resist is  $f_{ck}$ ; and (2) The steel yields at a stress of  $f_y$ .

### A: Limit analysis of solid CFST sections under pure bending

The bending stresses, forces and moments on solid circular and square sections at the limit stage are calculated and summarized in Table 1.

Table 1 Limit analysis of pure bending of solid CFST sections

Actions	Solid circular CFST section	Solid square CFST section
Distribution of stress at the limit stage		
Forces in concrete and steel	$F_{cc} = f_{ck} R^2 (\pi/2 - \gamma_0 - \sin(2\gamma_0)/2)$ $F_{sc} = f_y t R (\pi - 2\gamma_0)$ $F_{st} = f_y t R (\pi + 2\gamma_0)$	$F_{cc} = f_{ck} B^2 (1 - k_0) / 2$ $F_{sc} = f_y t B (2 - k_0)$ $F_{st} = f_y t B (2 + k_0)$
Moment about horizontal axis of symmetry	$M_{cc} = \frac{2}{3} f_{ck} R^3 \cos^3 \gamma_0$ $M_{st} = M_{sc} = 2 f_y R^2 t \cos \gamma_0$	$M_{cc} = \frac{1}{8} f_{ck} B^3 (1 - k_0^2)$ $M_{st} = M_{sc} = \frac{1}{2} f_y t B^2 + \frac{1}{4} f_y t B^2 (1 - k_0^2)$

The definition of the symbols used in the Table 1 and the following calculations can be found in the Notation Section presented before Introduction. The location of plastic neutral axis can be obtained by considering force equilibrium, i.e.,  $F_{st} = F_{sc} + F_{cc}$ . Thus, the following equations are obtained, respectively, for the circular and square sections.

a) Circular CFST:

$$\xi_{sc} = \frac{1}{2\gamma_0} \left( \frac{\pi}{2} - \gamma_0 - \frac{1}{2} \sin(2\gamma_0) \right) \quad (1)$$

b) Square CFST: •

$$k_0 = \frac{f_{ck} B^2}{4 f_y t B + f_{ck} B^2} \approx \frac{1}{\xi_{sc} + 1} \Rightarrow \xi_{sc} \approx \frac{1}{k_0} - 1 \quad (2)$$

Where  $\gamma_0$  is the location angle of plastic neutral axis as shown in Table 1 for a circular section, and  $k_0$  is the location ratio of plastic neutral axis as shown in Table 1 for a square section.

The ultimate moment of the sections can be obtained by  $M_u = M_{cc} + 2M_{sc}$ . For the circular and square sections, they are, respectively:

a) Circular CFST:

$$M_u = \frac{2}{\pi} \left( \frac{\cos^3 \gamma_0}{3 \xi_{sc}} + \cos \gamma_0 \right) f_y A_s R = k_c f_y A_s R \quad (3a)$$

Where

$$k_c = \frac{2}{\pi} \left( \frac{\cos^3 \gamma_0}{3 \xi_{sc}} \right) + \cos \gamma_0 \quad (3b)$$

b) Square CFST:

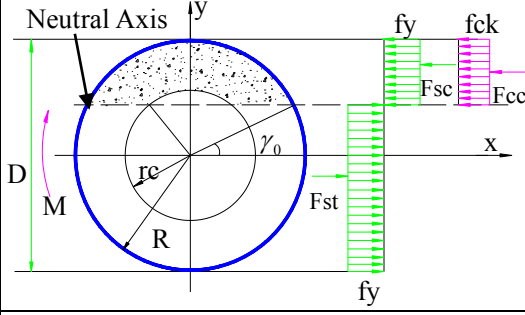
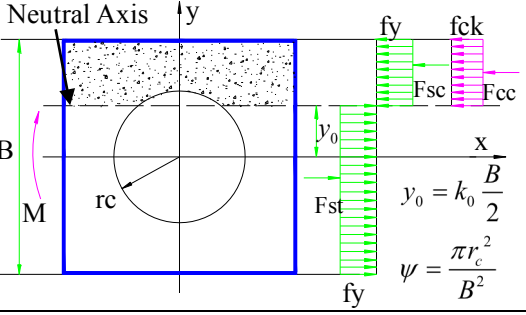
$$M_u \approx \left(1 - \frac{1}{4} \frac{\xi_{sc}}{\xi_{sc} + 1}\right) f_y A_s \frac{B}{2} = k_s f_s A_s = k_s f_y A_s \frac{B}{2} \quad (4a)$$

Where 
$$k_s = 1 - \frac{1}{4} \frac{\xi_{sc}}{\xi_{sc} + 1} \quad (4b)$$

### B: Limit analysis of hollow CFST sections under pure bending

For a hollow section, when the plastic neutral axis does not cross the hollow area, the formulas for ultimate moment of the section are the same as Eq.(3) and (4). Otherwise, the bending stresses, forces and moments on a hollow circular and square sections at the limit stage are calculated and summarized in Table 2.

Table 2 Limit analysis of pure bending of hollow CFST section

Actions	Hollow circular CFST section	Hollow square CFST section
Distribution of stress at the limit stage		
Forces in concrete and steel	$F_{cc} = f_{ck} R^2 (\pi/2 - \gamma_0 - \sin(2\gamma_0)/2)$ $- f_{ck} r_c^2 \times \left( \pi/2 - \arcsin\left(\frac{R}{r_c} \sin(\gamma_0)\right) - \frac{1}{2} \sin\left(2 \arcsin\left(\frac{R}{r_c} \sin(\gamma_0)\right)\right) \right)$ $F_{sc} = f_y t R (\pi - 2\gamma_0)$ $F_{st} = f_y t R (\pi + 2\gamma_0)$	$F_{cc} = f_{ck} B^2 (1 - k_0) / 2 - f_{ck} r_c^2 \times \left( \frac{\pi}{2} - \arcsin\left(\frac{k_0 B}{2r_c}\right) - \frac{1}{2} \sin\left(2 \arcsin\left(\frac{k_0 B}{2r_c}\right)\right) \right)$ $F_{sc} = f_y t B (2 - 2k_0)$ $F_{st} = f_y t B (2 + 2k_0)$
Moment about horizontal axis of symmetry	$M_{cc} = \frac{2}{3} f_{ck} R^3 \left( \cos^3 \gamma_0 - \psi \sqrt{\psi} \times \cos^3 \left( \arcsin\left(\frac{\sin \gamma_0}{\sqrt{\psi}}\right) \right) \right)$ $M_{st} = M_{sc} = 2 f_y R^2 t \cos \gamma_0$	$M_{cc} = \frac{1}{8} f_{ck} B^3 (1 - k_0^2) - \frac{2}{3} f_{ck} B^3 \frac{\psi}{\pi} \sqrt{\frac{\psi}{\pi}} \cos^3 \left( \arcsin\left(\sqrt{\frac{\pi}{\psi}} \frac{k_0}{2}\right) \right)$ $M_{st} = M_{sc} = \frac{1}{2} f_y t B^2 + \frac{1}{4} f_y t B^2 (1 - k_0^2)$

Again, the location of plastic neutral axis is determined by considering force equilibrium, i.e.,  $F_{st} = F_{sc} + F_{cc}$ . The solid confining coefficients of circular and square sections are, respectively:

a) For circular CFST, when  $\sin \gamma_0 \leq \sqrt{\psi}$ :

$$\xi_{sc} = \frac{1}{2\gamma_0} \left( \frac{\pi}{2} - \gamma_0 - \frac{1}{2} \sin(2\gamma_0) \right) - \frac{\psi}{2\gamma_0} \times \left( \frac{\pi}{2} - \arcsin\left(\frac{\sin \gamma_0}{\sqrt{\psi}}\right) - \frac{1}{2} \sin\left(2 \arcsin\left(\frac{\sin \gamma_0}{\sqrt{\psi}}\right)\right) \right) \quad (5)$$

b) For Square CFST, when  $k_0 \leq 2\sqrt{\frac{\psi}{\pi}}$  :

$$\xi_{sc} \approx \frac{1}{k_0} - 1 - \frac{2}{k_0} \frac{\psi}{\pi} \times \left( \frac{\pi}{2} - \arcsin\left(\sqrt{\frac{\pi}{\psi}} \frac{k_0}{2}\right) - \frac{1}{2} \sin\left(2 \arcsin\left(\sqrt{\frac{\pi}{\psi}} \frac{k_0}{2}\right)\right) \right) \quad (6)$$

Similar to the case of solid CFST, the ultimate bending moment of CFST columns with hollow circular and square sections can be calculated, respectively, as:

a) Circular CFST, when  $\sin \gamma_0 \leq 2\sqrt{\psi}$  :

$$M_u = \frac{2}{\pi} \left( \frac{1}{3\xi_{sc}} \left( \cos^3 \gamma_0 - \psi \sqrt{\psi} \times \cos^3 \left( \arcsin \left( \frac{\sin \gamma_0}{\sqrt{\psi}} \right) \right) \right) + \cos \gamma_0 \right) f_y A_s R = k_c f_y A_s R \quad (7)$$

$$\text{Where } k_c = \frac{2}{\pi} \left( \frac{1}{3\xi_{sc}} \left( \cos^3 \gamma_0 - \psi \sqrt{\psi} \times \cos^3 \left( \arcsin \left( \frac{\sin \gamma_0}{\sqrt{\psi}} \right) \right) \right) + \cos \gamma_0 \right)$$

b) Square CFST, when  $k_0 \leq 2\sqrt{\frac{\psi}{\pi}}$  :

$$M_u = \left( \frac{1}{4} \left( \frac{1}{\xi_{sc}} + 1 \right) (1 - k_0^2) + \frac{1}{2} - \frac{4}{3\xi_{sc}} \frac{\psi}{\pi} \cos^3 \sqrt{\frac{\psi}{\pi}} \left( \arcsin \left( \sqrt{\frac{\pi}{\psi}} \frac{k_0}{2} \right) \right) \right) f_y A_s \frac{B}{2} = k_s f_y A_s \frac{B}{2} \quad (8)$$

$$\text{Where } k_s \approx \left( \frac{1}{4} \left( \frac{1}{\xi_{sc}} + 1 \right) (1 - k_0^2) + \frac{1}{2} - \frac{4}{3\xi_{sc}} \frac{\psi}{\pi} \cos^3 \sqrt{\frac{\psi}{\pi}} \left( \arcsin \left( \sqrt{\frac{\pi}{\psi}} \frac{k_0}{2} \right) \right) \right)$$

Where  $\xi_{sc}$  denotes confining coefficient of solid section,  $\xi_{sc} = A_s f_y / (A_c + A_k) f_{ck}$ ;  $f_y$  and  $A_s$  represent the strength and area of steel tube, respectively;  $f_{ck}$  and  $A_c$  are the respective strength and area of steel tube; and  $A_k$  is the area of hollow, i.e., for a solid section  $A_k = 0$ .

## 2.2 Unified formulation of the ultimate bending moment of solid and hollow CFST sections

### A: Unified formulation of solid CFST sections under pure bending

For a solid section, the two factors,  $k_c$  and  $k_s$ , calculated from equations (3b) and (4b) against a range of solid confining coefficient  $\xi_{sc}$  are show in Figure 1. It is seen that when  $\xi_{sc} \geq 0.5$ , which is the case of most practical design, the curves of  $k_c$  and  $k_s$  are virtually parallel to each other. Thus, the ultimate moment of a square section can be taken as the one of an equivalent circular section that is converted from the square section by following the procedure below.

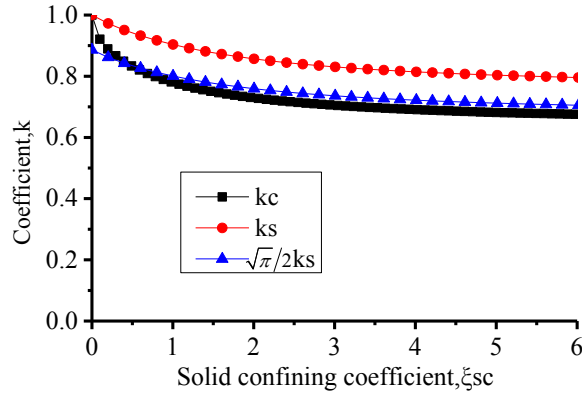


Figure 1. Factor k against confining coefficient

Assume that the square section of side B has the same cross sectional area as a circular section of radius  $\bar{R}$ . Thus

$$B^2 = \pi \bar{R}^2 \quad \text{and} \quad \frac{B}{2} = \frac{\sqrt{\pi}}{2} \bar{R} \quad (9)$$

For the square section (see equation(4))

$$M_u = k_s f_y A_s \frac{B}{2} = \left( \frac{\sqrt{\pi}}{2} k_s \right) f_y A_s \bar{R} \quad (10)$$

Considering the above equivalency, the ultimate bending moment of a solid CFST section with either a circular or a square section can be written in a unified form as

$$M_u = k f_y A_s \bar{R} \quad (11)$$

where  $\bar{R}$  denotes the radius of a circular section or the equivalent radius of a square section calculated from equation (9). The coefficient  $k$  for a square section is calculated from equation (10). In order to further simplify and unify equation(10), the  $k_s$  and  $k_c$  curves are compared with the  $\sqrt{\pi}/2 \cdot k_s$  curve in Figure 1. It can be clearly seen that the  $\sqrt{\pi}/2 \cdot k_s$  curve representing the equivalent circular section is very close to  $k_c$ . As a result, the simple formula of  $k_s$  (equation (4b)) can be approximately used for both square and circular sections.

From the above analysis, the unified formulation of ultimate bending moment for a solid CFST with either a circular or a square section is given by:

$$M_u = \frac{\sqrt{\pi}}{2} \left( 1 - \frac{1}{4} \frac{\xi_{sc}}{\xi_{sc} + 1} \right) f_y A_s \bar{R} \quad (12)$$

## B: Unified formulation of solid and hollow CFST sections under pure bending

It can be seen from equations (3), (4), (7) and (8) that  $k_c$  (for circulate section) and  $k_s$  (for square section) are functions of solid confining coefficient  $\xi_{sc}$  and hollow ratio  $\psi$  that are all related to the unified confining coefficient  $\xi$  by:

$$\xi = \frac{A_s f_y}{A_c f_{ck}} = \frac{\xi_{sc}}{1 - \psi} \quad (13)$$

Therefore, both  $k_c$  and  $k_s$  can be considered as functions of confining coefficient  $\xi$  and hollow ratio  $\psi$ . Figure 2 plots the two factors against a range of confining coefficient  $\xi$  and  $\psi$  that are commonly used in practical design.

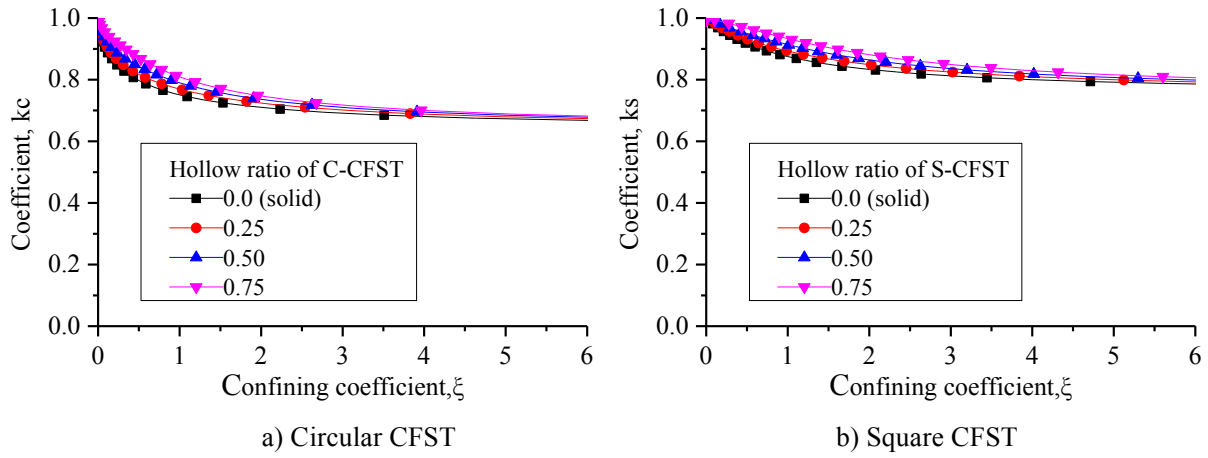


Figure 2 Coefficient k against confining coefficient  $\xi$  for various hollow ratios

The curves in Figure 2 show that for any practical values,  $\xi$ , the hollow ratio,  $\psi$ , does not have significant effect on the values of  $k_c$  and  $k_s$ . This observation suggests that equation (12) can be revised by replacing the solid confining coefficient  $\xi_{sc}$  with the confining coefficient  $\xi$  and extended to include hollow sections. Therefore, the unified formulation of the ultimate bending moment of CFST columns with solid and hollow sections is given by:

$$M_u = \frac{\sqrt{\pi}}{2} \left( 1 - \frac{1}{4} \frac{\xi}{\xi + 1} \right) f_y A_s \bar{R} \quad (14)$$

where  $\xi$  is confining coefficient, i.e.,  $\xi = A_s f_y / A_c f_{ck}$ ;  $\bar{R}$  is the radius of a circular section or the radius of an equivalent circular section converted from a square section;  $f_y$  and  $A_s$  represent the strength and area of steel tube, respectively.

### 2.3 Experimental verification and comparative analysis

Experimental results of solid CFST columns with circular [10, 11, 25] and square [25-32] sections under axial compression at room temperature from other researchers are used here to verify the accuracy and applicability of equation (14). The test results and the predictions from equation (14) are compared and shown in Table 3.

Table 3 Comparison of equation (14) with test results for circular sections

Type	Ref.	Test number		Geometric parameters		Material		Tests	Eq (14).	Ratio
		NO.	Numbering	Diameter	Thickness	$f_y$ /Mpa	$f_{ck}$ /Mpa	$M_{test}$ /kN*m	$M_c$ /kN*m	$M_c/M_{test}$
				D/mm	t/mm					
Circular CFST	[11]	1	CBC0-C	109.9	1.00	400	19.5	7.6	5.94	0.78
		2	CBC0-B	110.4	1.25	400	19.5	9.1	7.36	0.81
		3	CBC0-A	110.9	1.50	400	19.5	11	8.77	0.80
		4	CBC1	101.83	2.53	365	19.5	11.33	10.83	0.96
		5	CBC2	88.64	2.79	432	19.5	10.86	10.36	0.95
		6	CBC3	76.32	2.45	415	19.5	6.92	6.48	0.94
		7	CBC4	89.26	3.35	412	19.5	10.47	11.85	1.13
		8	CBC5	60.65	2.44	433	19.5	3.78	4.15	1.10
		9	CBC6	76.19	3.24	456	19.5	9.87	9.09	0.92
		10	CBC7	60.67	3.01	408	19.5	4.75	4.74	1.00
		11	CBC8	33.66	1.98	442	19.5	0.9	1.02	1.13

[25]	12	CBC9	33.78	2.63	460	19.5	1.17	1.37	1.17	
	13	CVA-1	100	1.90	282	57	9.19	6.79	0.74	
	14	CVA-2	100	1.90	282	57	7.33	6.79	0.93	
	15	CSCA-1	100	1.90	282	57	7.74	6.79	0.88	
	16	CB1-1	140	3.00	235	33.3	19.8	16.97	0.86	
	17	CB1-2	140	3.00	235	33.3	21.6	16.97	0.79	
	18	CB2-1	140	3.00	235	33.3	21.5	16.97	0.79	
	19	CB2-2	140	3.00	235	33.3	22.1	16.97	0.77	
	20	CB3-1	140	3.00	235	33.3	20.7	16.97	0.82	
	21	CB3-2	140	3.00	235	33.3	20.4	16.97	0.83	
	22	CB4-1	180	3.00	235	40.1	33.9	28.98	0.85	
	23	CB4-2	180	3.00	235	40.1	34.9	28.98	0.83	
	24	CB5-1	180	3.00	235	40.1	32.2	28.98	0.90	
	25	CB5-2	180	3.00	235	40.1	40.6	28.98	0.71	
	26	CB6-1	180	3.00	235	40.1	36.2	28.98	0.80	
	27	CB6-2	180	3.00	235	40.1	36.3	28.98	0.80	
	[10]	28	D1t1M20	44.45	1.25	250	18.626	0.74	0.71	0.95
		29	D1t2M20	44.45	1.60	250	18.626	1.08	0.88	0.81
		30	D1t3M20	44.45	2.00	250	18.626	1.23	1.07	0.87
		31	D2t1M20	57.15	1.25	250	18.626	1.42	1.20	0.84
		32	D2t2M20	57.15	1.60	250	18.626	1.76	1.49	0.85
		33	D2t3M20	57.15	2.00	250	18.626	2.25	1.82	0.81
		34	D3t1M20	63.5	1.25	250	18.626	1.8	1.49	0.83
		35	D3t2M20	63.5	1.60	250	18.626	2.18	1.86	0.85
		36	D3t3M20	63.5	2.00	250	18.626	2.82	2.28	0.81
		37	D1t1M30	44.45	1.25	250	28.14	0.89	0.73	0.82
		38	D1t2M30	44.45	1.60	250	28.14	1.16	0.90	0.78
39		D1t3M30	44.45	2.00	250	28.14	1.39	1.10	0.79	
40		D2t1M30	57.15	1.25	250	28.14	1.57	1.23	0.78	
41		D2t2M30	57.15	1.60	250	28.14	1.98	1.54	0.78	
42		D2t3M30	57.15	2.00	250	28.14	2.52	1.87	0.74	
43		D3t1M30	63.5	1.25	250	28.14	2.03	1.54	0.76	
44		D3t2M30	63.5	1.60	250	28.14	2.55	1.92	0.75	
45		D3t3M30	63.5	2.00	250	28.14	3.16	2.34	0.74	
46		D1t1M40	44.45	1.25	250	34.17	0.86	0.74	0.86	
47		D1t2M40	44.45	1.60	250	34.17	1.19	0.92	0.77	
48		D1t3M40	44.45	2.00	250	34.17	1.46	1.12	0.76	
49		D2t1M40	57.15	1.25	250	34.17	1.54	1.25	0.81	
50		D2t2M40	57.15	1.60	250	34.17	2.03	1.56	0.77	
51		D2t3M40	57.15	2.00	250	34.17	2.55	1.90	0.75	
52		D3t1M40	63.5	1.25	250	34.17	2.03	1.56	0.77	
53		D3t2M40	63.5	1.60	250	34.17	2.71	1.95	0.72	
54		D3t3M40	63.5	2.00	250	34.17	3.31	2.38	0.72	

Table 4 Comparison of equation (14) with test results for square section

Type	Ref.	Test number		Geometric parameters		Material		Tests	Eq.(14)	Ratio	
		NO.	Numbering	Length of side	Steel thickness	$f_y$ /Mpa	$f_{ck}$ /Mpa	$M_{test}$ /kN*m	$M_c$ /kN*m	$M_c/M_{test}$	
				B/mm	t/mm						
Square CFST	[26]	1	RB1-1	120	120	3.84	330.1	18.29	29.34	28.98	0.99
		2	RB2-1	120	120	3.84	330.1	23.58	30.16	29.46	0.98
		3	RB2-2	120	120	3.84	330.1	23.58	32.25	29.46	0.91
		4	RB2-3	120	120	3.84	330.1	23.58	31.69	29.46	0.93
		5	RB3-1	120	120	5.86	321.1	20.97	40.90	41.52	1.02
		6	RB3-2	120	120	5.86	321.1	20.97	41.54	41.52	1.00
		7	RB4-1	120	120	5.86	321.1	26.80	41.43	42.10	1.02
		8	RB4-2	120	120	5.86	321.1	26.80	42.61	42.10	0.99
	[27]	9	CB12	152	152	4.80	389.0	63.20	73.60	73.89	1.00



	10	CB13	152	152	4.80	389.0	41.00	75.10	71.64	0.95
	11	CB15	152	152	4.80	389.0	35.80	71.30	70.96	1.00
	12	CB22	152	152	9.50	432.0	62.40	146.50	147.55	1.01
[28]	13	HS6	126	126	3.00	300.0	40.30	27.90	24.87	0.89
	14	HS12	156	156	3.00	300.0	40.30	42.40	38.89	0.92
	15	NS6	186	186	3.00	300.0	26.10	62.60	54.55	0.87
	16	NS12	246	246	3.00	300.0	31.00	103.50	98.73	0.95
	17	NS18	306	306	3.00	300.0	31.00	153.00	155.13	1.01
[29]	18	HSS6	110	110	5.00	750.0	24.50	66.00	67.87	1.03
	19	HSS13	160	160	5.00	750.0	24.50	141.00	148.37	1.05
	20	HSS19	210	210	5.00	750.0	26.10	228.00	262.55	1.15
[25]	21	SVA-1	100	100	1.90	282.0	57.00	10.83	9.76	0.90
	22	SVA-2	100	100	1.90	282.0	57.00	9.96	9.76	0.98
	23	SSCA-1	100	100	1.90	282.0	57.00	10.33	9.76	0.94
	24	SVB-1	200	200	1.90	282.0	57.00	42.30	40.73	0.96
	25	SVB-2	200	200	1.90	282.0	57.00	54.94	40.73	0.74
	26	SSCB-1	200	200	1.90	282.0	57.00	56.70	40.73	0.72
	27	SB1-1	140	140	3.00	235.0	40.10	31.90	24.68	0.77
	28	SB1-2	140	140	3.00	235.0	40.10	27.50	24.68	0.90
	29	SB2-1	140	140	3.00	235.0	40.10	29.40	24.68	0.84
	30	SB2-2	140	140	3.00	235.0	40.10	25.90	24.68	0.95
	31	SB3-1	140	140	3.00	235.0	40.10	30.20	24.68	0.82
	32	SB3-2	140	140	3.00	235.0	40.10	29.40	24.68	0.84
	33	SB4-1	180	180	3.00	235.0	40.10	37.60	41.64	1.11
	34	SB4-2	180	180	3.00	235.0	40.10	43.10	41.64	0.97
	35	SB5-1	180	180	3.00	235.0	40.10	37.90	41.64	1.10
36	SB5-2	180	180	3.00	235.0	40.10	41.70	41.64	1.00	
37	SB6-1	180	180	3.00	235.0	40.10	49.80	41.64	0.84	
38	SB6-2	180	180	3.00	235.0	40.10	46.50	41.64	0.90	
[30]	39	B01	150	150	4.88	438.0	53.54	81.80	80.56	0.98
	40	B02	150	150	4.87	438.0	53.54	88.10	80.64	0.92
	41	B03	150	150	4.92	438.0	74.23	98.40	83.18	0.85
	42	B04	150	150	4.84	438.0	74.23	101.40	81.86	0.81
[31]	43	32LM-SB	175	175	3.20	299.0	28.76	71.79	51.11	0.71
	44	45LM-SB	175	175	4.50	295.0	28.76	110.15	68.64	0.62
	45	60LM-SB	175	175	6.00	285.0	28.76	129.82	85.90	0.66
	46	32HM-SB	175	175	3.20	299.0	38.32	71.85	52.11	0.73
	47	45HM-SB	175	175	4.50	295.0	38.32	109.12	70.06	0.64
	48	60HM-SB	175	175	6.00	285.0	38.32	130.71	87.68	0.67
[32]	49	1	220	220	4.00	293.8	20.10	71.30	96.89	1.36
	50	3	350	350	4.00	293.8	20.10	212.40	255.47	1.20
	51	6	280	280	4.00	293.8	20.10	140.70	160.44	1.14
	52	7	150	150	2.95	319.3	71.92	34.94	38.53	1.10
	53	8	151	151	4.86	316.6	71.92	68.03	61.15	0.90

The error analyses of the comparisons in Tables 3 and 4 are shown in Figure 3 where all the 54 circular members and 53 square members are included. For the circular members, the average and variance of the prediction to the test result ratios are 0.84 and 0.01, respectively. For the square members, they are respectively 0.93 and 0.02. The overall average of the ratios for both sections is 0.885. The underestimated ultimate bending moment from the predictions are mainly attributed to the fact that strain-hardening of steel was ignored in the above analytical analysis. This will be further discussed in the next section.

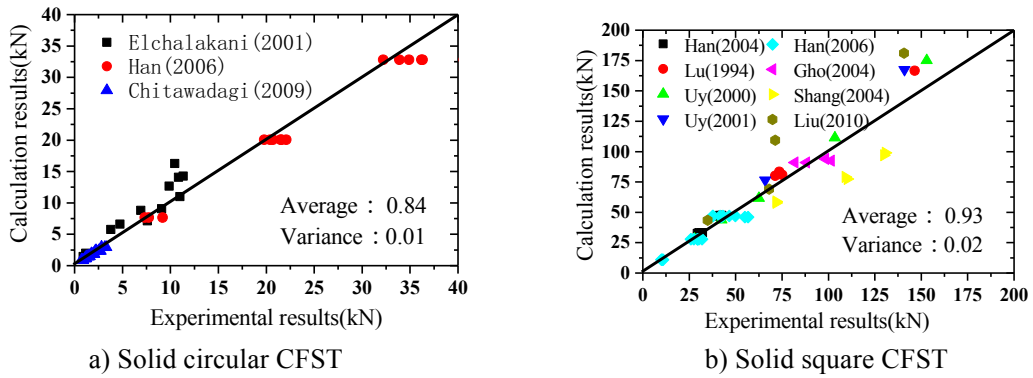


Figure 3 Comparison of the unified formula calculations and tests results

It is observed that the constant coefficient,  $\sqrt{\pi}/2$ , in equation (14) is close to the average of the ratios shown in the last column of Tables 3 and 4, which is 0.885. It is proposed, therefore, that  $\sqrt{\pi}/2$  can be removed from Eq.(14) to achieve a better average of the prediction to test result ratio. Hence, the unified formulation of ultimate bending moment of CFST column can be further revised as:

$$M_u = \left( 1 - \frac{1}{4} \frac{\xi}{\xi + 1} \right) f_y A_s \bar{R} \quad (15)$$

For hollow sections, since there are no experimental test results available for comparisons, the predictions from equation (15) are compared with independent FE simulations<sup>[33]</sup>. Similar error analyses to Figure 3 are conducted. The comparisons show that for the hollow circular sections, the average and variance of the prediction to test result ratios are 0.95 and 0.01, respectively, and for the hollow square sections, they are, respectively, 1.05 and 0.03.

To further verify the above formula, numerical simulation results<sup>[33]</sup> of 24 square hollow CFST columns and 24 hollow CFST columns with octagonal section subjected to bending are compared with the predictions of equation (15). Figure 4 shows the average and variance of the ratio that are 1.01 and 0.005 for square section and 1.05 and 0.007 for octagonal section. Clearly, the simple formula has shown very good agreement with both the test and numerical results of other researchers.

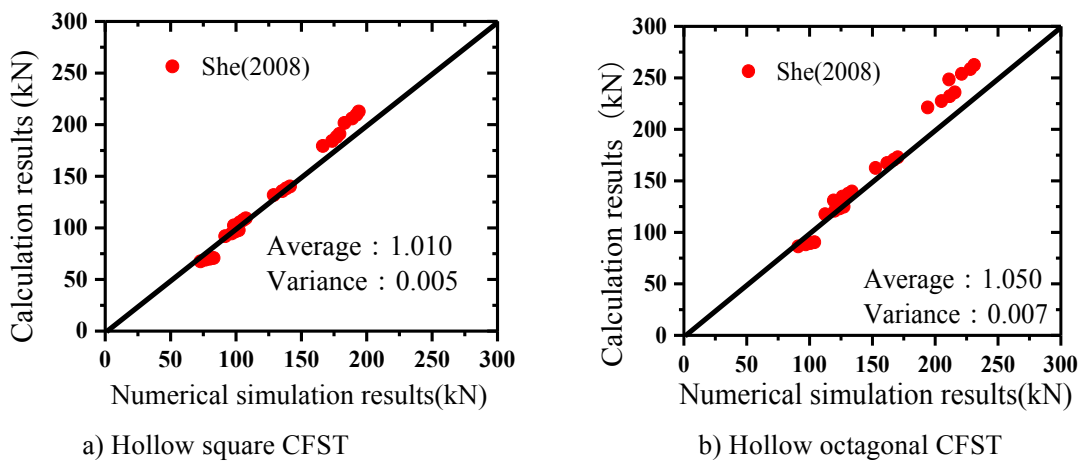


Figure 4 Comparison of the unified formula calculations and test results

### 3 Ultimate bending moment of concrete-filled steel tube at elevated temperature

#### 3.1 Fire resistance of CFST under bending using finite element method

Using the equivalent area approach, the analyses presented in the above sections provided a unified formulation for the ultimate bending moment of circular and polygonal CFST sections subjected to room temperature. It was observed that the theoretical predictions of Eq.(14) were conservative, which was attributed to the fact that the strain hardening of the steel tube was ignored. In order to evaluate the applicability of the equivalent area method and the effect of strain hardening of steel when CFST columns are subjected to elevated temperature or fire conditions, finite element results are used in this section to validate the formula predictions.

The following steps are followed in the FEM simulations: Step 1: calculate the temperature field of CFST under standard fire by heat transfer analysis; Step 2: import the calculated time dependent temperature field from Step 1 starting from the room temperature at the initial time, calculate the moment-rotation curve of the CFST column under bending, thus the ultimate bending moment of the CFST column, and Step 3: repeat previous steps over a period of time at every single time step to plot the ultimate bending moment. Solid elements were used in the finite element model and more details of the models can be found in references [25-28], where the thermal properties of concrete and steel were taken from EC4. The constitutive law of the concrete was also taken from EC4, while the stress-strain relation of steel was simplified by the bilinear model shown in Figure 5. In the FE calculations, both  $E_{c,T} = 0.01E_T$  and  $E_{c,T} = 0.0$  were considered.

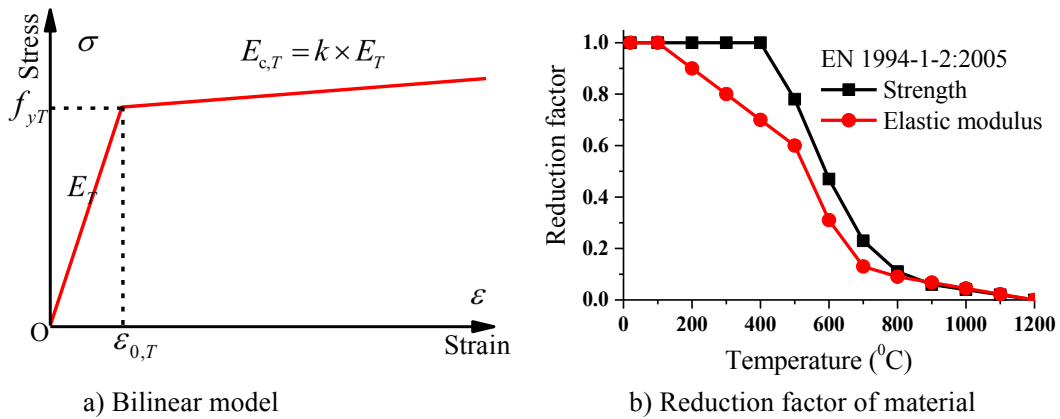


Figure 5 Thermal and mechanical properties of steel

Parameters that affect fire resistance of CFST columns include geometry, material properties and loading conditions, e.g., the shape of CFST section, thickness of steel tube, hollow ratio, grade of steel and concrete, and fire curves and exposure time, etc. In this study, the fire curve used in the FE simulation followed ISO-834 standard. The geometry and materials of the circular CFST columns were chosen from the most-commonly ones used in practical engineering design. The range of the external diameter,  $D$ , of the steel tube, the thickness of the tube,  $d$ , and the hollow ratio,  $\psi$ , were, respectively, between 200 mm~1200 mm, 3 mm~18 mm and 0.0~0.65. The grade of steel and concrete were respectively Q235~Q460 and C30~C80. For the square and octagonal CFST sections, their respective equivalent circular sections were considered by following the equivalent area approach. To compare the formula predictions with the numerical simulations, 5 design parameters were considered for all the CFST sections, each of which took 6 different values that are uniformly distributed within the specified ranges, as shown in Table 5. To further reduce the number of test samples without loss of generality, uniform design experimentation was adopted to select representative designs from Table 5 for validation. The selected designs are shown in Table 6.

Table 5 The parameters and design of CFST under fire

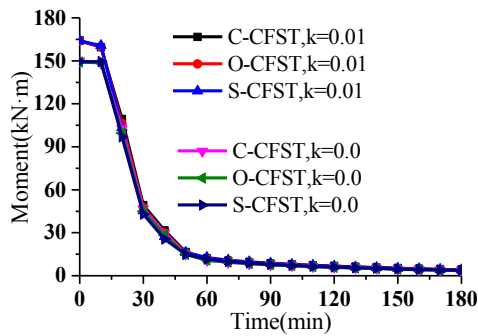
Parameters	Values before uniform design experimentation					
	1	2	3	4	5	6
Equivalent diameter $D$ /mm	200	400	600	800	1000	1200

Equivalent thickness d/mm	3	6	9	12	15	18
Hollow ratio $\psi$	0	0.25	0.35	0.45	0.55	0.65
Steel grade	Q235	Q295	Q345	Q390	Q420	Q460
Concrete grade	C30	C40	C50	C60	C70	C80

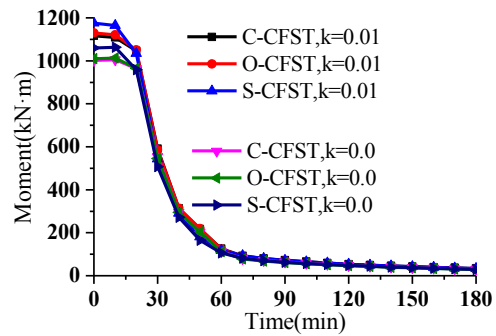
Table 6 Uniform design experimentation results of the selected design

Numbering	Selected design after uniform design experimentation				
	Equivalent diameter D	Equivalent thickness d	Hollow ratio $\psi$	Steel grade	Concrete grade
No.13142	1 (200mm)	3 (9mm)	1 (0.00)	4 (Q390)	2 (C40)
No.26436	2 (400mm)	6 (18mm)	4 (0.45)	3 (Q345)	6 (C80)
No.31654	3 (600mm)	1 (3mm)	6 (0.65)	5 (Q420)	4 (C60)
No.44511	4 (800mm)	4 (12mm)	5 (0.55)	1 (Q235)	1 (C30)
No.52225	5 (1000mm)	2 (6mm)	2 (0.25)	2 (Q295)	5 (C70)
No.65363	6 (1200mm)	5 (15mm)	3 (0.35)	6 (Q460)	3 (C50)

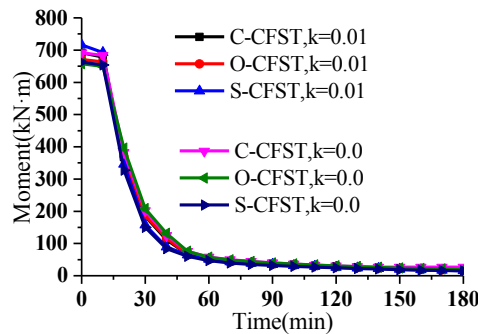
By following the FE simulation procedure mentioned above, the ultimate bending moment of the CFST columns with circular (C), square (S) and octagonal (O) sections are shown in Figure 6, respectively, for the 6 selected designs specified in Table 6.



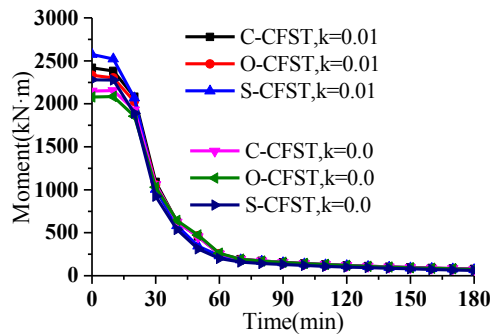
a) No.13142



b) No.26436



c) No. No.31654



d) No. No.44511

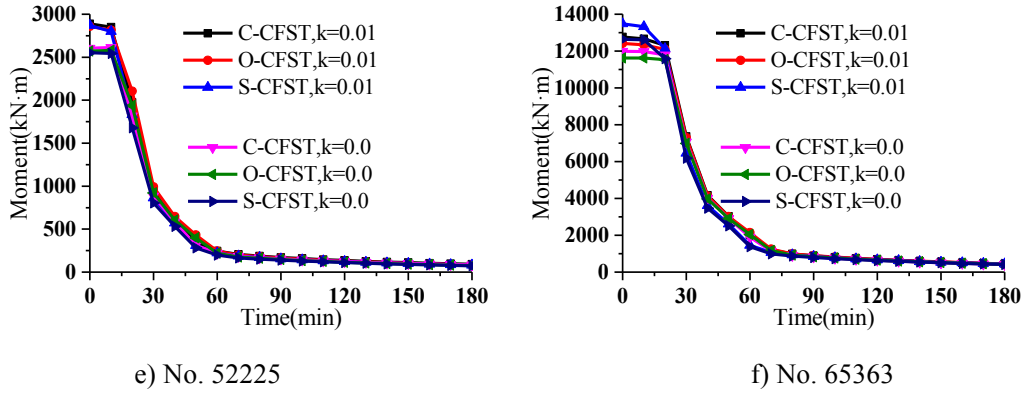


Figure 6 Bending capacity vs time for CFST

From the above numerical simulations, it can be observed that (a) the ultimate bending moment is higher when strain hardening ( $k=0.01$ ) is considered, especially when a CFST column is subjected to room temperature, which explains why the ultimate bending moments calculated in the previous section, where  $k=0$  was assumed, is lower than the test results; (b) the predicted ultimate bending moments of the square and octagonal sections using the equivalent area approach are very close to those of their equivalent circular sections, especially when the columns are subjected to high temperature; and (c) the patterns of all the curves are very similar giving an ultimate bending moment reduction of about 90% after 60 minutes under fire.

### 3.2 Unified formulation for ultimate bending moment of CFST columns under fire

From the authors' previous work<sup>[34]</sup>, it has been concluded that for a CFST column subjected to axial compression, the compressive strength of the column subjected to fire can be calculated from the formula of the same column under the room temperature by replacing the respective strength of material and elastic modules under the room temperature with the ones obtained from the average temperature approach, so that the application of the formulas can be extended directly to include elevated temperature, where the average temperature of a polygonal section is calculated from its equivalent circular section. The FE results presented in Figure 6 have shown that the equivalent area approach worked well for calculating ultimate bending moment of CFST columns under fire. It was also noticed that when a CFST column is under fire, its ultimate bending moment is determined mainly by the ultimate bending moment of the steel tube. Therefore, on the basis of Eq.(15), the unified method for calculating ultimate bending moment of CFST columns under fire can be written as:

$$M_{u, T} = \left(1 - \frac{1}{4} \frac{\xi_T}{\xi_T + 1}\right) f_{y, \bar{T}_s} A_s \bar{R} \quad (16)$$

where  $\bar{R}$  is the radius of a circular section or the radius of an equivalent circular section converted from a square section;  $\xi_T$  represents the standard value of confining coefficient at high temperature, i.e.,  $\xi_T = A_s f_{y, \bar{T}_s} / A_c \bar{f}_{ck, \bar{T}_s}$ , and the equivalent strength of concrete and steel are, respectively<sup>[34]</sup>:

$$f_{y, \bar{T}_s} = k_{s, T}(\bar{T}_s) f_y \quad (17)$$

$$\bar{f}_{ck, \bar{T}_c} = \bar{k}_{c, T}(\bar{T}_c) f_{ck} \quad (18)$$

In Eqs (17) and (18),  $k_{s, T}$  denotes the reduction factor of steel strength as a function of temperature;  $\bar{k}_{c, T}$  denotes the reduction factor of concrete strength, also, as a function of temperature that can be calculated respectively by<sup>[34]</sup>.

$$\bar{k}_{s,T}(\bar{T}_s) = \frac{f_{y,T}}{f_y} = \begin{cases} 1 & 20^\circ C \leq \bar{T}_s \leq 400^\circ C \\ e^{-\left(\frac{\bar{T}_s-400}{240}\right)^5} & 400^\circ C \leq \bar{T}_s \leq 1200^\circ C \end{cases} \quad (19)$$

$$\bar{k}_{c,T}(\bar{T}_c) = 1 - \frac{\bar{T}_c - 20}{918}, 0 \leq \bar{k}_{c,T} \leq 1 \quad (20)$$

where  $\bar{T}_s$  and  $\bar{T}$  are the average temperature of steel tube and concrete, respectively. More details of the average temperature approach can be found from reference<sup>[34]</sup>.

Figure 7 shows comparisons between the predictions from Eq.(16) and the FE simulation for test sample No.26436. In Figure 7 a, the ultimate bending moment of the CFST columns having circular, square and octagonal sections with and without steel strain hardening are plotted against fire exposure time. The comparisons are presented in Figure 7b for the ultimate bending moment of the CFST columns when the fire exposure time is below 60 minutes. It can be found that the average ratio of the prediction to the FEA results is 0.872, with a variance of 0.028. The comparisons have demonstrated the applicability of the developed unified formula for both circular and polygonal sections, and for both room and elevated temperature.

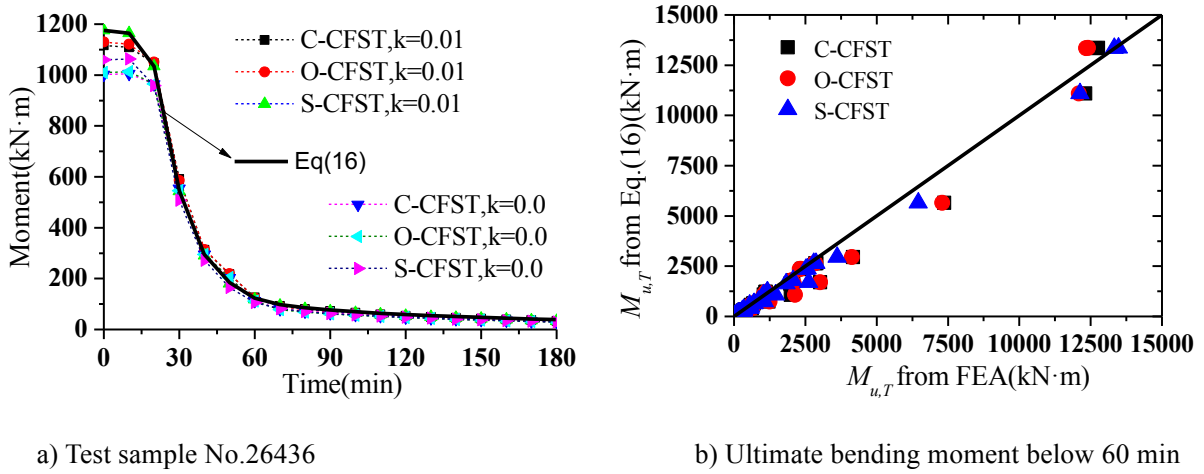


Figure 7 Comparison between results of formula (Eq.16) and FEM simulation

It should be mentioned here that the calculation of the average temperature followed the same principles described in [34], as it is commonly accepted that the mechanical and the temperature fields can be independently analysed in construction design. Therefore the average temperature was calculated regardless of the loading conditions. Evidently, the above evaluations and comparison have confirmed the suitability of the average temperature method for bending analyses of CFST columns.

### 3.3 Restrictions on the application of the formulas and discussion

It is evident that for solid and hollow CFST columns with various sectional profiles, Eq.(16) can provide a unified formulation to cover a wide range of temperature starting from the room temperature. However, it is worthwhile to note that the restrictions on the application of the unified fire resistance formulas depend on the applicability of using average temperature of the steel tube and concrete in the calculation. The proposed calculation method using average temperature can be applied (but may not be limited) to the analysis of ultimate bending moment of CFST columns satisfying the following conditions:

- Diameter or equivalent diameter of cross-section:  $120\text{mm} \leq \bar{D}(2\bar{R}) \leq 2000\text{mm}$ ;
- Fire resistance time:  $t \leq 4\text{hours}$ ;
- Hollow ratio:  $0 \leq \psi \leq 0.75$ ;

(d) Normal weight concrete: C30~C80 and structural steel: Q235~Q420.

## 4 Concluding remarks

Based on the limit analysis, the ultimate bending moment of circular and square CFST columns of solid and hollow sections subjected to bending only were derived, from which a unified formula was developed to predict the ultimate bending moment under room temperature. The formula was validated by comparing the predictions with existing test and numerical results.

The unified formula was then extended to include CFST columns subjected to fire by following the average temperature approach proposed by the authors in previous studies<sup>[34]</sup>. The predictions from the extended unified formula were compared with finite element analyses, where the effect of steel strain hardening was considered. The validations demonstrated that the unified formula could be used in the design of a range of CFST columns subjected to room temperature and fire conditions.

Further work is needed to extend the current method to columns subjected to combined loading, and also to CFST columns with fire protection. The development of the formula for average temperature to include lightweight concrete and some other special type of concrete or steel is also possible.

## Acknowledgement

The authors are grateful for the financial support from the National Natural Science Foundation of China (Grant No.51508425), the Natural Science Foundation of Hubei Province, China (Grant No.2015CFB171) and the Fundamental Research Funds for the Central Universities (Grant No.2042014kf0010).

## References

- [1] Han L, Li W, Bjorhovde R. Developments and Advanced Applications of Concrete-Filled Steel Tubular (CFST) Structures: Members. *Journal of Constructional Steel Research*, 2014,100:211-228.
- [2] Yu Z W, Ding F X, Cai C S. Experimental Behavior of Circular Concrete-Filled Steel Tube Stub Columns. *Journal of Constructional Steel Research*, 2007,63(2):165-174.
- [3] Uy B, Tao Z, Liao F Y, et al. Behaviour of Slender Square Concrete-Filled Stainless Steel Columns Subject to Axial Load//The eleventh Nordic Steel Construction Conference, NSCC2009, Malmö, sweden, 2009:359-366.
- [4] Tao Z, Wang Z, Yu Q. Finite Element Modelling of Concrete-Filled Steel Stub Columns under Axial Compression. *Journal of Constructional Steel Research*, 2013,89:121-131.
- [5] Choi K K, Xiao Y. Analytical Studies of Concrete-Filled Circular Steel Tubes under Axial Compression. *Journal of Structural Engineering*, 2010,136(5):565-573.
- [6] Dai X, Lam D. Numerical Modelling of the Axial Compressive Behaviour of Short Concrete-Filled Elliptical Steel Columns. *Journal of Constructional Steel Research*, 2010,66(4):542-555.
- [7] Ding F, Li Z, Cheng S, et al. Composite Action of Octagonal Concrete-Filled Steel Tubular Stub Columns Under Axial Loading. *Thin-Walled Structures*, 2016,107:453-461.
- [8] Yu M, Zha X, Ye J, et al. A Unified Formulation for Hollow and Solid Concrete-Filled Steel Tube Columns Under Axial Compression. *Engineering Structures*, 2010,32(4):1046-1053.
- [9] Dai X H, Lam D, Jamaluddin N, et al. Numerical Analysis of Slender Elliptical Concrete Filled Columns Under Axial Compression. *Thin-Walled Structures*, 2014,77:26-35.
- [10] Chitawadagi M V, Narasimhan M C. Strength Deformation Behaviour of Circular Concrete Filled Steel Tubes Subjected to Pure Bending. *Journal of Constructional Steel Research*, 2009,65(8-9):1836-1845.
- [11] Elchalakani M, Zhao X L, Grzebieta R H. Concrete-Filled Circular Steel Tubes Subjected to Pure Bending. *Journal of Constructional Steel Research*, 2001,65(8):1836-1845.

- [12] Yu Q, Tao Z, Chen Z, et al. Flexural Behavior of Steel Tube Confined Concrete Members Under Pure Bending. 2008,25(3):187-193.(in Chinese)
- [13] Moon J, Roeder C W, Lehman D E, et al. Analytical Modeling of Bending of Circular Concrete-Filled Steel Tubes. *Engineering Structures*, 2012,42:349-361.
- [14] Fa-Xing D, Zhi-Wu Y U. Pure Bending Properties of Self-Compacting Concrete Filled Circular Steel Tube. *Journal of Traffic and Transportation Engineering*, 2006,6(1):63-68, 79.(in Chinese)
- [15] Nie J, Wang Y, Fan J. Experimental Research on Concrete Filled Steel Tube Columns under Combined Compression-Bending-Torsion Cyclic Load. *Thin-Walled Structures*, 2013,67:1-14.
- [16] Portolés J M, Romero M L, Bonet J L, et al. Experimental Study of High Strength Concrete-Filled Circular Tubular Columns Under Eccentric Loading. *Journal of Constructional Steel Research*, 2011,67(4):623-633.
- [17] Choi Y, Foutch D A, Lafave J M. New Approach to AISC P-M Interaction Curve for Square Concrete Filled Tube (CFT) Beam-Columns. *Engineering Structures*, 2006,28(11):1586-1598.
- [18] Kodur V K R, Mackinnon D H. Simplified Design of Concrete-Filled Hollow Structural Steel Columns for Fire Endurance. *Journal of Constructional Steel Research*, 1998,51(1):21-36.
- [19] Li G Q, He J L, Han L H. Load bearing Capacity of Fire resistance of Concrete Filled Steel Tubular Columns. *Building Structure*, 2001,31(01):60-62.(in Chinese)
- [20] Tan K H, Tang C Y. Interaction Model for Unprotected Concrete Filled Steel Columns Under Standard Fire Conditions. *Journal of Structural Engineering*, 2004,130(9):1405-1413.
- [21] Espinos A, Romero M L, Hospitaler A. Simple Calculation Model for Evaluating the Fire Resistance of Unreinforced Concrete Filled Tubular Columns. *Engineering Structures*, 2012,42:231-244.
- [22] Espinos A, Romero M L, Hospitaler A. Fire Design Method for Bar-Reinforced Circular and Elliptical Concrete Filled Tubular Columns. *Engineering Structures*, 2013,56:384-395.
- [23] EN 1994-1-2:2005. Design of Composite Steel and Concrete Structures Part 1.2: General Rules, Structural Fire Design, Brussels[S]. British Standards Institution, 2005.
- [24] Yu M, Zha X X, Ye J Q, et al. A Unified Formulation for Circle and Polygon Concrete-Filled Steel Tube Columns under Axial Compression. *Engineering Structures*, 2012,49:1-10.
- [25] Han L H, Lu H, Yao G, et al. Further Study on the Flexural Behaviour of Concrete-Filled Steel Tubes. *Journal of Constructional Steel Research*, 2006,62(6):554-565.
- [26] Han L H. Flexural Behavior of Concrete-Filled Steel Tubes. *Journal of Constructional Steel Research*, 2004,60(2):313-337.
- [27] Lu Y Q, Kennedy DJL. The Flexural Behavior of Concrete-Filled Hollow Structural Sections. *Canadian Journal of Civil Engineering*, 1994.
- [28] Uy B. Strength of Concrete Filled Steel Box Columns Incorporating Local Buckling. *Journal of Structural Engineering*, 2000,126(3):341-352.
- [29] Uy B. Strength of Short Concrete Filled High Strength Steel Box Columns. *Journal of Constructional Steel Research*, 2001,24(6):575-582.
- [30] Gho W M, Liu D L. Flexural Behavior of High-Strength Rectangular Concrete-Filled Steel Hollow Sections. *Journal of Constructional Steel Research*, 2004.
- [31] Shang Z Q. Study on Mechanical Properties of Plain Concrete and Reinforced Concrete-filled Steel Tube Beams and Columns. *Shenyang University of Technology*, 2004.(in Chinese)
- [32] Liu X, Wu Y B. Experiment and Simulation Analysis of Bearing Capacity of Concrete-Filled Rectangular Steel Tube Beam. *Industrial Construction*, 2010,40(7):91-94, 104.(in Chinese)
- [33] She C Y. Research on the Strength and Stability of Hollow Polygonal Concrete-filled Steel Tubes. *Harbin Institute of Technology*, 2008.(in Chinese)
- [34] Yu M, Zha X, Ye J, et al. A Unified Method for Calculating Fire Resistance of Solid and Hollow Concrete-Filled Steel Tube Columns Based on Average Temperature. *Engineering Structures*, 2014,71:12-22.